Clouds of High Contrast on Uranus

Erich Karkoschka

Near-infrared images of Uranus taken with the Hubble Space Telescope in July and October 1997 revealed discrete clouds with contrasts exceeding 10 times the highest contrast observed before with other techniques. At visible wavelengths, these 10 clouds had lower contrasts than clouds seen by Voyager 2 in 1986. Uranus' rotational rates for southern latitudes were identical in 1986 and 1997. Clouds in northern latitudes rotate slightly more slowly than clouds in opposite southern latitudes.

Voyager 2 discovered discrete cloud features on Uranus (1). The contrast of those eight clouds ranged from less than 1% in the violet to 7% in the red (Table 1), where the contrast is the relative enhancement of albedo over the underlying belt or zone. Two near-infrared (NIR) images taken in 1994 with the Hubble Space Telescope (HST) showed two clouds of about 12% contrast (2). Compared to the other jovian planets, the small number of clouds on Uranus and their low contrast have hampered our understanding of its atmospheric dynamics.

Forty-three images of Uranus were taken during five orbits of HST in July and October 1997 with the Wide Field/Planetary Camera 2 (WFPC2) and the Near Infrared Camera and Multi-Object Spectrometer (NICMOS) in the wavelength range from 0.24 to 2.03 μm. Ten clouds (labeled A through J in Fig. 1) were detected. Several clouds have contrasts exceeding 100%. The clouds are not much larger than HST's point spread function, corresponding to 1000 km at full width at half maximum in the visible and 2500 km at 2-μm wavelength. The diameters of the clouds (Table 2) were estimated by comparison of the observed intensity profile with synthetic instrumental point spread functions smeared by various degrees and these sizes are upper limits. Lower limits of the cloud sizes are at least 500 km smaller and are less certain. Clouds A through H appear to be circular, whereas clouds I and J are long streaks that are similar to clouds observed by Voyager 2 (1).

At visible wavelengths, the clouds are spatially resolved so that sizes and contrasts can be measured directly. However, near 2-μm wavelength, the smallest clouds appear almost as point sources. The product of contrast and area can be measured, but each quantity cannot be measured separately. Assuming that the sizes measured at shorter wavelengths remained the same at longer wavelengths and that the contrast is constant across the disk of each cloud, modeled contrasts were inferred. HST's point spread function at 2 μm degrades the contrast of a 2000-km-diameter cloud by a factor of almost 10 (somewhat dependent on the foreshortening), whereas this factor is less than 2 at 0.7 μm. Clouds are labeled according to decreasing maximum modeled contrast (Table 2), which occurs near 1.8-μm wavelength except for cloud G, which was only observed at wavelengths less than 1 μm. Because the sizes are upper limits, the derived modeled contrasts are lower limits. A smaller assumed size will shift the contrast upward without changing its dependence on the wavelength (Fig. 2). Cloud I looks like a 30° stretch of the brightest zone displaced by 2° toward the equator. However, its dependence of contrast on wavelength is closer to that of clouds H and J than to that between zones. Therefore, it is called a cloud rather than a wave in the zonal boundary.

Although the results of this work are based on NIR images rich in features (Fig. 1, C through E), the observing program also included several filters similar to filters in the Voyager cameras (wavelengths 0.35 to 0.62 μm). These HST images are almost bland (Fig. 1, A and B) and are similar to views by Voyager. No clouds were seen in these HST images with the exception of cloud J, detected as a dark feature (–3% contrast) at 0.34-μm wavelength. Near 0.8-μm wavelength, clouds were seen in the southern hemisphere as in 1994, but more faintly than observed previously. An image taken by Hammel in 1997 at 0.62-μm wavelength did show one cloud of low contrast (3). The current observations were taken when the southern hemisphere's activity was rather low. The apparent increase in contrast (Table 1) is not due to increased atmospheric activity. It is due to expansion of the spectral range and to the recent emergence from darkness of the apparently more active northern hemisphere (4).

The basic physical characteristics of the clouds can be estimated. Bright clouds of optical depth 0.1 give an albedo enhancement of ~0.1 at most NIR wavelengths, as long as gaseous absorption above the clouds is negligible (top dashed line in Fig. 2). Within the wavelength range from 0.7 to 1.6 μm, each cloud shows an almost constant albedo enhancement of <0.1. From 1.6 to 2.0 μm, the albedo enhancement drops steeply by two orders of magnitude to values on the order of 0.0001 (bottom dashed line in Fig. 2). This indicates strong gaseous absorption above the cloud tops. Using current models of the atmosphere of Uranus (5, 6), the wavelength and size of this dropoff put the cloud tops somewhere

Table 1. The four measurements of the contrast of clouds on Uranus that increased the maximum measured contrast.

Date	Instrument	Wavelength (μm)	Contrast (%)
January 1986	Voyager 2	0.62	7
14 August 1994	HST (WFPC2)	0.78	12
25 July 1997	HST (WFPC2)	0.91	25
28 July 1997	HST (NICMOS)	1.87	180

Table 2. Maximum contrasts, sizes (width and length are given for clouds I and J), latitudes, and observation periods of 10 uranian clouds. Dashes indicate that the cloud was on the night side during the observation.

Cloud	Maximum contrast (%)		Diameter (10^3 km)	Latitude (°)	Date in 1997				
	Imaged	Modeled			July				October
A	120	900	2	+28	–	25	28	29	–
B	130	750	2	+27	–	25	28	29	–
C	180	600	2.5	+28	–	–	28	–	–
D	120	250	3.5	+30	–	–	28	–	–
E	50	120	3	+29	–	–	28	–	–
F	35	60	2.5	+17	–	–	28	–	16
G	10	25	1.5	+27	–	25	–	29	–
H	18	25	2.5	–25	–	25	28	29	–
I	9	20	1 × 10	–42	–	25	28	–	16
J	8	15	1 × 10	–31	7	25	28	29	–

Lunar and Planetary Laboratory, University of Arizona, Tucson, AZ 85721–0092, USA. E-mail: erich@pirl.lpl.arizona.edu

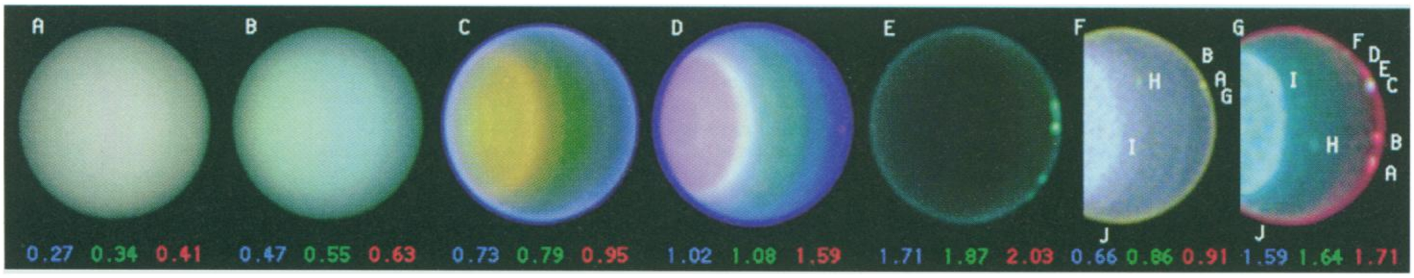

Fig. 1. Seven false-color images made from 21 HST exposures of Uranus with 19 different filters. Panel (**B**) is close to the true color. Wavelengths are given in micrometers. The cameras WFPC2 and NICMOS covered wavelengths below and above 1.05 μm, respectively. All 15 exposures used for (**A**) through (**E**) were processed in the same way, allowing a direct comparison over a wide spectral range. In order to show all 10 clouds, the zonal brightness was mostly subtracted in (**F**) and (**G**) (*11*). Clouds D and F are almost behind the limb in (G) but are more prominent in (E), where cloud D is the top bright one and the faint cloud F is to its upper left.

near the 0.5-bar level, about a scale height (~25 km) above the suspected methane (CH_4) cloud layer at 1.3 bar. The large NIR contrasts of up to 900% are due to CH_4 absorption, causing low zonal albedos while the cloud tops lie above most of the CH_4.

Models (*5, 6*) indicate aerosols above the 0.5-bar level with an optical depth on the order of 0.001 at 1.6 μm; aerosol radii at 0.5 bar are about 0.3 μm. The scattering efficiency of such aerosols drops by a factor of 6 from 0.7 to 1.6 μm. The observed clouds do not show such a decrease of optical depth, which indicates larger aerosols, possibly similar to aerosols of the CH_4 cloud layer, which are believed to be 1 μm or larger in radius.

The contrast reversal between ultraviolet (UV) and NIR wavelengths observed for cloud J is common in atmospheres with gaseous opacity dominated by Rayleigh scattering in the UV and by CH_4 absorption in the NIR (*7, 8*). The same contrast reversal also occurs in a southern mid-latitude zone on Uranus.

The four bright clouds (A, B, C, and D) rotated counterclockwise by about 30° over 1.4 hours (the time elapsed between the taking of images E and G in Fig. 1). The differential rotation of Uranus can be visualized by comparing images F and G in Fig. 1, taken 66 hours apart. Cloud J has almost completed four rotations during this time interval. Cloud I has moved ahead of cloud J, indicating a faster rotation. The remaining clouds have fallen behind their position in Fig. 1F, indicating a slower rotation.

Rotational periods for seven clouds (Fig. 3) were determined from 90 positional measurements. Rotational periods for the three southern clouds H, I, and J agree with data obtained by Voyager 2 (Fig. 3), indicating that the rotation rates in southern latitudes in 1986 and 1997 were identical. On the other hand, Hammel concluded from two HST data points (Fig. 3) that the rotational period probably changed between 1986 and 1994 (*9*). Because the deviations are less than twice the error bars, it is also possible that Uranus' rotation rate has remained constant. The 1997 observations are 10 times more accurate than the 1994 observations because the observing program lasted 3 months, as compared with only 8 hours in 1994. Voyager 2 detected clouds during a 10-day period. If clouds exhibit spatial variations on shorter time scales below the limit of resolution, the 1994 data can yield only momentary motions, whereas the 1986 and 1997 data give long-term averages.

Northern latitudes, invisible in 1986

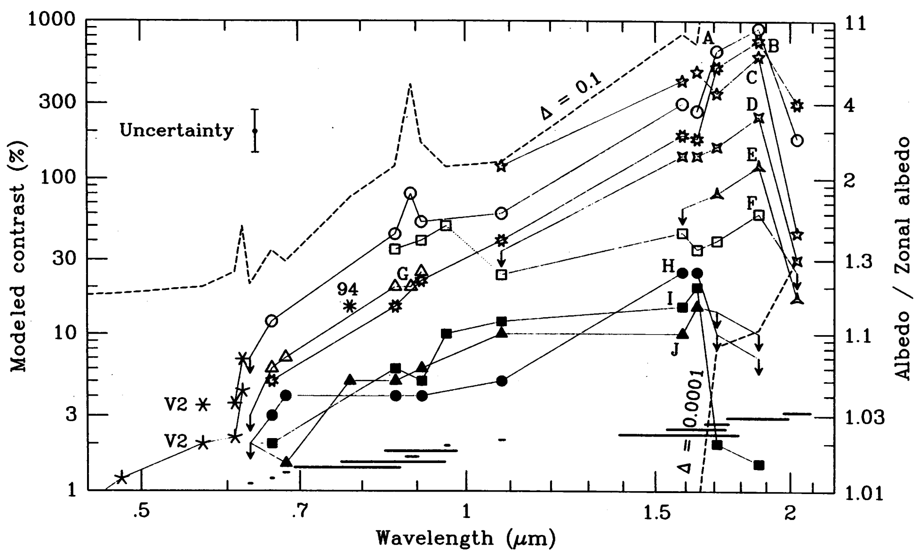

Fig. 2. The contrast of clouds on Uranus as a function of wavelength. Data from this work obtained with 14 filters are compared with the very limited amount of all previous data collected by Voyager 2 (symbols marked V2) and by HST in 1994 (symbol marked 94). The southern and northern clouds of 1997 are indicated by solid and open symbols, respectively. Modeled contrasts are shown for all HST data, whereas no correction was applied to Voyager data. Upper limits are indicated by down-pointing arrows. The relative uncertainty of 30% shown at the upper left refers to the products of contrast and area. Filter widths are marked at the bottom. For comparison, the dashed lines display the contrast for absolute albedo enhancements Δ of 0.1 and 0.0001.

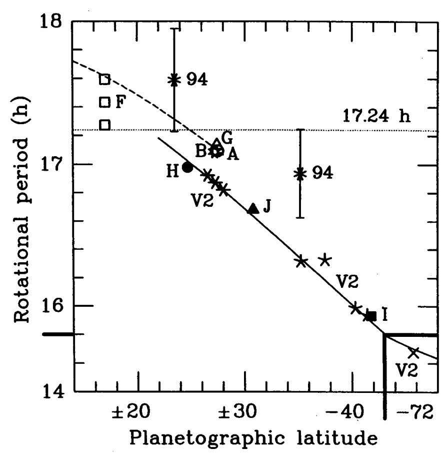

Fig. 3. Rotational periods of clouds on Uranus. Measurements from this work for both hemispheres are compared with previous data confined to the southern hemisphere. Symbols are the same as in Fig. 2. The uncertainties of the new data points are as large as the sizes of the symbols. The curves show fitted rotational profiles, solid for the southern hemisphere and dashed for the northern hemisphere. The interior rotates once every 17.24 hours.

(4), are sampled by clouds A, B, F, and G. They consistently rotate more slowly than clouds in southern latitudes. Both hemispheres follow different rotational curves (Fig. 3), separated by five times the uncertainty of the data. The data are consistent with symmetry relative to a latitude of 2°N. Because of insufficient temporal coverage for cloud F, the solution for its rotational period yields three possible values (Fig. 3). The longest period follows the apparent trend and is thus preferred. Cloud F, closest to the equator, may be an indicator of tropical activity.

The 15 investigated clouds of 1986 and 1997 range over 100° of latitude and 3.3 hours of rotational period. Their rotational period can be fitted by a smooth curve to only 0.04 hour standard deviation. Such a function without an attached physical significance is $(482 - 8 \sin \phi + 127 \sin^2 \phi)°$/day, where ϕ is the latitude (Fig. 3). It predicts an equatorial rotational period of 17.9 hours, which is consistent with Voyager's radio occultation measurement that yielded 18.0 ± 0.3 hours (*10*).

All seven clouds with measured rotational periods (A, B, F, G, H, I, and J) were observed whenever they were on the illuminated side of the disk. There is no evidence for the appearance or disappearance of a cloud during the 100-day observation interval. Of course, it is possible that one cloud disappeared and another one emerged at a similar location during the long intervals without observation. Observations of cloud F at wavelengths below 1 μm came 80 days after its observations at longer wavelengths. Its unusual negative slope at 1 μm (Fig. 2) may be an indication of change rather than a spectral feature. Cloud G may have faded somewhat during its 4-day observation interval.

REFERENCES AND NOTES

1. B. A. Smith *et al.*, *Science* **233**, 43 (1986).
2. P. K. Seidelman *et al.*, Space Telescope Science Institute (STScI) press release PR94–50 (STScI, Baltimore, MD, 1994).
3. H. B. Hammel *et al.*, STScI press release PR97–36 (STScI, Baltimore, MD, 1997).
4. The subsolar point of Uranus moved from 82° to 40° south between 1986 and 1997, beginning to illuminate the northern hemisphere.
5. K. Rages *et al.*, *Icarus* **89**, 359 (1991).
6. K. H. Baines *et al.*, *ibid.* **114**, 328 (1995).
7. E. Karkoschka and M. G. Tomako, *ibid.* **106**, 428 (1993).
8. R. D. Lorenz *et al.*, *ibid.* **127**, 173 (1997).
9. H. B. Hammel, *Bull. Am. Astron. Soc.* **29**, 994 (1997).
10. G. F. Lindal *et al.*, *J. Geophys. Res.* **92**, 14987 (1987).
11. The zonal brightness was determined in two steps. First, the data numbers of pixel pairs oriented symmetrically to the central meridian were replaced by their minimum, with the assumption that only bright discrete features exist and that features are not located symmetrically to the central meridian. Second, data further than 0.2″ from the limb were fitted to a linear function of the cosine of the emission angle.

12. This work was based on observations made with the NASA/European Space Agency HST, obtained at the Space Telescope Science Institute (STScI), which is operated by the Association of Universities for Research in Astronomy under NASA contract NAS5–26555. Support was provided by NASA through grant number GO-07429.01–97A from STScI. I thank M. Tomasko for his support and the crew at STScI for their cooperation with special requests for scheduling and implementation. The NICMOS camera team made these observations possible.

7 November 1997; accepted 3 March 1998

Brain Activity During Speaking: From Syntax to Phonology in 40 Milliseconds

Miranda van Turennout,* Peter Hagoort, Colin M. Brown

In normal conversation, speakers translate thoughts into words at high speed. To enable this speed, the retrieval of distinct types of linguistic knowledge has to be orchestrated with millisecond precision. The nature of this orchestration is still largely unknown. This report presents dynamic measures of the real-time activation of two basic types of linguistic knowledge, syntax and phonology. Electrophysiological data demonstrate that during noun-phrase production speakers retrieve the syntactic gender of a noun before its abstract phonological properties. This two-step process operates at high speed: the data show that phonological information is already available 40 milliseconds after syntactic properties have been retrieved.

From early in life we acquire knowledge about the words in our language. This knowledge includes information about the meaning of words, their syntactic properties (such as word class), and their phonological properties (such as their phonemes and syllable structure). All this information is stored in a component of long-term memory that is usually referred to as the mental lexicon. During speaking, the mental lexicon is accessed automatically at very high speed to select words that express the intended meaning, and to retrieve their syntactic and phonological properties. These properties are used to structure the words according to the syntactic constraints of one's language and to build up the sound pattern of an utterance. A central unresolved question concerns the orchestration in real time of the retrieval of the distinct types of linguistic knowledge required to produce fluent speech (*1*, *2*). The activation of this knowledge necessarily precedes articulation, but only by a fraction of a second, given the speed with which we speak. Data from behavioral studies as well from neuropsychological studies of patients with language impairment have suggested that a word's semantic and syntactic properties are retrieved before its phonological form is constructed (*2*, *3*). We have now obtained direct evidence on the real time activation of syntax and phonology in Dutch noun-phrase production. We found that the syntactic gender of a noun is retrieved about 40 ms earlier than its first phonological segment.

Max Planck Institute for Psycholinguistics, Wundtlaan 1, 6525 XD Nijmegen, The Netherlands.

*To whom correspondence should be addressed at Laboratory of Brain and Cognition, National Institute of Mental Health, Building 10, Room 4C104, 10 Center Drive MSC 1366, Bethesda, MD 20892–1366, USA.

The main experimental task was the production of noun phrases in Dutch. Participants (*4*) were presented with colored pictures of objects and animals, which they were instructed to name using a noun phrase without a definite article (such as "rode tafel," red table). On half of the trials they performed a syntactic-phonological classification task before producing the noun phrase. The classification task consisted of the conjunction of a go/no-go decision and a left- or right-hand response. In the first experiment, the response hand was determined by the syntactic classification, and the phonological classification determined whether or not a push-button response should be given (Fig. 1) (*5*). The syntactic and phonological properties of the word that are required to perform the classification tasks become available automatically through the speech production system. The syntactic classification involved determining the gender of the noun. In Dutch, as in, for example, French and German, nouns are characterized by syntactic gender. This is a purely syntactic property that needs to be retrieved from the mental lexicon during noun-phrase production to determine the definite article of the noun ("de" for common gender, and "het" for neuter gender), or the adjectival suffix when no definite article is used in the noun phrase ("-e" for common gender, and no suffix for neuter gender). The phonological classification involved determining the word-initial pho-